

Hot Corrosion Behavior of Thermal Spray Coating

by

Karabo Masipa

15218

Dissertation submitted in partial fulfillment of
the requirements for the
Bachelor of Engineering (Hons)
(Mechanical Engineering)

JANUARY 2015

Universiti Teknologi PETRONAS
Bandar Seri Iskandar
31750 Tronoh
Perak Darul Ridzuan

CERTIFICATION OF APPROVAL

Hot Corrosion Behavior of Thermal Spray Coating

by

Karabo Masipa

15218

Dissertation submitted in partial fulfillment of
the requirements for the
Bachelor of Engineering (Hons)
(Mechanical Engineering)

Approved by,

Dr Subhash Kamal (Supervisor)

Universiti Teknologi PETRONAS
TRONOH, PERAK
January 2015

CERTIFICATION OF ORIGINALITY

This is to certify that I am responsible for the work submitted in this project, that the original work is my own except as specified in the references and acknowledgements, and that the original work contained herein has not been undertaken or done by unspecified sources or persons.

KARABO MASIPA

ABSTRACT

Austenitic stainless steel AISI 304 and Boiler steels (such as P11, P22, P12) find their largest application in the manufacturing industry. These are preferred because of their superior mechanical strength, surface stability, creep and fatigue resistance. However, they are highly susceptible to hot corrosion. Therefore, surface engineering imparts hot corrosion resistance properties in high temperature corrosive environments. In the present study, Cr_3C_2 -25NiCr coating was deposited on the substrate 304SS by High Velocity Oxygen Fuel (HVOF) technique in order to investigate the behavior of the Cr_3C_2 -NiCr thermal spray coating. The bare specimens were boiler steel alloys P11, P12 and P22. Hot corrosion test was conducted on bare and coated specimens in 40% K_2SO_4 -40% Na_2SO_4 -10%NaCl -10%KCl environment at 900 °C for 10 cycles. Corrosion kinetics was monitored using weight gain measurements. Characterization of corrosion products was carried out by scanning electron microscope with energy-dispersive x-ray spectroscopy (SEM/EDS) technique. The observed corrosion resistance of the Cr_3C_2 -NiCr coating can be attributed to the formation of protective oxide scale Cr_2O_3 . The corrosion mechanism of the coating is discussed.

ACKNOWLEDGEMENTS

First and foremost I would like to thank God the Almighty for the completion of this project.

The implementation of this project would not have been possible without the support of many individuals. Therefore I would like to extend my sincere gratitude to all of them.

I am thankful to Dr Subhash Kamal for his support and providing me with the necessary guidance throughout the project.

I am also grateful to the Laboratory Technologists for provision of expertise and technical support during the experimentations. Without their expertise, the project would lack in quality of outcomes, thus their support has been essential.

I am indebted to my loving family for their unending support and encouragement in my career path. They have been supporting me financially, spiritually and otherwise, which helped me in the completion of this project.

TABLE OF CONTENTS

TITLE PAGE	i
CERTIFICATION OF APPROVAL	ii
CERTIFICATION OF ORIGINALITY	iii
ABSTRACT	iv
ACKNOWLEDGEMENT	v
LIST OF FIGURES	viii
LIST OF TABLES	ix
ABBREVIATIONS	x
CHAPTER 1: INTRODUCTION	1
1.1 Background of Study.....	1
1.2 Problem Statement	3
1.3 Objectives	3
1.4 Scope of the Project.....	4
CHAPTER 2: LITERATURE REVIEW	5
CHAPTER 3: METHODOLOGY	10
3.1 Substrate Materials	10
3.2 Sample Preparation	10
3.3 Corrosion Test.....	11
3.4 Characterization Techniques	11
CHAPTER 4: RESULTS AND DISCUSSION	12
4.1 Visual Observation.....	13
4.2 Weight Change Measurements.....	13
4.3 Morphology and Composition of Scales	14

4.4	Discussion	17
CHAPTER 4:	CONCLUSION AND RECOMMENDATION	19
REFERENCES		20
APPENDICES		22

LIST OF FIGURES

Figure 1: Basic Principle of Thermal Spraying [6]	2
Figure 2: Coating deposition and the oxidation process [12].....	3
Figure 3: FESEM micrograph of coating powders (a) $\text{Cr}_3\text{C}_2\text{-25NiCr}$, (b) $\text{Cr}_3\text{C}_2\text{-25(NiCr)+0.4\%CeO}_2$, (c) $\text{Cr}_3\text{C}_2\text{-25(NiCr)+0.4\%CeO}_2$ with EDS [17].....	7
Figure 4: Macrophotos of (a) Superni 600, (b) Superni 718, and (c) Superco 605 after cyclic hot corrosion in $\text{Na}_2\text{SO}_4\text{-25\%NaCl}$ at 900°C for 100 cycles [14].....	8
Figure 5: Macrographs of specimens after cycle 1; a) P11, b) P12, c) P22 and d) $\text{Cr}_3\text{C}_2\text{-NiCr}$ coated specimen	13
Figure 6: Macrographs of specimens at cycle 10; a) P11, b) P12, c) P22 and d) $\text{Cr}_3\text{C}_2\text{-NiCr}$ coated specimen	13
Figure 7: Weight change curves for bare and $\text{Cr}_3\text{C}_2\text{-NiCr}$ coated specimens.....	14
Figure 8: SEM micrograph of hot corroded bare P11 surface	15
Figure 9: SEM micrograph of hot corroded bare P12 surface	15
Figure 10: SEM micrograph of hot corroded bare P22 surface	15
Figure 11: SEM micrograph of hot corroded $\text{Cr}_3\text{C}_2\text{-NiCr}$ coated surface	16
Figure 12: SEM micrographs of bare P11 hot corroded surface.....	22
Figure 13: SEM micrographs of bare P12 hot corroded surface.....	22
Figure 14: SEM micrographs of bare P22 hot corroded surface.....	22
Figure 15: SEM micrographs of bare P22 hot corroded surface.....	23

LIST OF TABLES

Table 1: Chemical Composition of the Materials	10
Table 2: Elements found in the hot corroded Cr_3C_2 -NiCr coated surface	16
Table 3: Project Milestone for FYP I.....	24
Table 4: Project Milestone for FYP II.....	24

ABBREVIATIONS

AISI – American Iron and Steel Institute

$\text{Cr}_3\text{C}_2\text{-NiCr}$ - Chromium carbide-Nickel chrome

HVOF – High Velocity Oxygen Fuel

SEM – Scanning Electron Microscope

XRD – X-ray diffraction

Na_2SO_4 – Sodium sulfate

NaCl – Sodium chloride

V_2O_5 – Vanadium pentoxide

SO_3 – Sulfur trioxide

LVOF – Low Velocity Oxygen Fuel

AIP – Arc ion plating

CHAPTER 1

1. INTRODUCTION

1.1. Background of Study

Engineering systems operating at high temperatures of above 650°C involve contact metallic materials with combustion product gases. This leads to the detrimental phenomenon of hot corrosion. Hot corrosion is the most aggressive form of degradation of components operating in high temperatures such as gas turbines, furnaces, boilers and diesel engines. It is an accelerated corrosion, resulting from the presence of salt contaminants such as Na_2SO_4 , NaCl and V_2O_5 that combine to form molten deposits [1]; consequently causing the dissolution of protective surface oxides at the metal surface, contributing to the weakening of the material as the surface is rapidly consumed.

Hot corrosion can be characterized into two types, i.e. Type I, also known as high temperature hot corrosion, is characterized by temperature range 800-950°C [1,6]; and Type II, also known as low temperature hot corrosion, occurring at temperatures below 800°C [3]. Type I corrosion is caused by molten salt deposition on the material surface, while Type II hot corrosion mechanism involves acidic fluxing of protective oxides by sulfur trioxides (SO_3) dissolved in molten sulfates [6].

Compounds such as sodium, vanadium, potassium and sulfur are common impurities that are present in many high temperature environments. They react together to form low melting molten salts that get deposited on the material surface as a thin film and induce hot corrosion [4, 5].

Components used in aggressive environments require materials capable of withstanding increasing operating temperatures, chemical degradation and with good mechanical properties. However, it is not possible for a single material to have different properties to meet today's industrial demand [4]. Therefore, the use of protective coatings on the material surface could enhance the material properties to

withstand the aggressive environments. Protective coating techniques such as thermal spraying and laser cladding have become more popular [4].

Thermal spray coating offers an effective and economic way to counteract the hot corrosion problem since it alters the surface without affecting any other properties of the components [4, 6]. Thermal spray coatings are produced by rapidly heating the feedstock material in a hot gaseous medium and simultaneously projecting it at a high velocity onto a prepared surface where it builds up to produce the desired coating [4]. There are various thermal spraying techniques that can be used to apply coating, such as plasma, detonation gun, high velocity oxygen fuel (HVOF), low velocity oxygen fuel (LVOF) and arc ion plating (AIP).

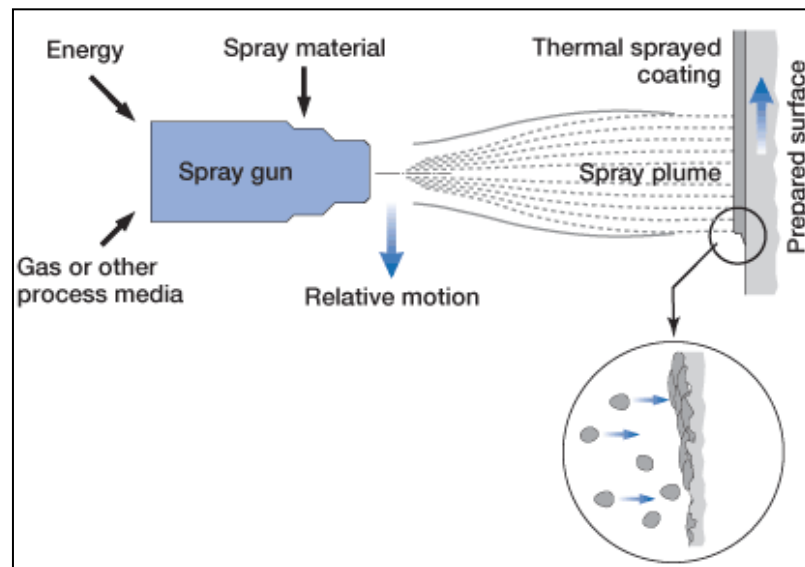


Figure 1: Basic Principle of Thermal Spraying [6]

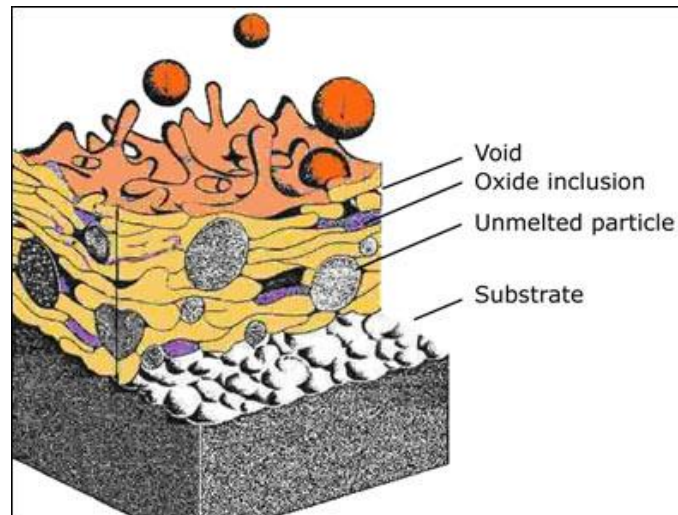


Figure 2: Coating deposition and the oxidation process [12]

1.2. Problem Statement

Austenitic stainless steel AISI 304 and Boiler steels (such as P11, P22, P12) find their largest application in the manufacturing industry; these are preferred because of their superior mechanical strength, surface stability, creep and fatigue resistance. Materials used for high temperature strength are highly susceptible to hot corrosion and the surface engineering plays a key role in effectively combating the hot corrosion and oxidation problems. The contaminants such as sodium, sulfur and vanadium cause the metals to undergo a rapid degradation. Consequently, the metals weaken and their life span is shortened, leading to the catastrophic failure of the components. This phenomenon occurs as a result of contaminants reacting with one another, forming molten salts that get deposited as a thin film on the metal surface. This is called hot corrosion and is a common occurrence in high temperature operating systems.

1.3. Objectives

The aim of this study is to investigate the behavior of bare and Cr_3C_2 -NiCr coated alloys under molten salts environment (40% K_2SO_4 -40% Na_2SO_4 -10% NaCl - 10% KCl) at of 900 °C for 50 hours (10 cycles).

1.4. Scope of Study

Hot corrosion is a serious problem, recent studies show that the high temperature strength materials are highly susceptible to hot corrosion and surface engineering plays a key role in effectively alleviating hot corrosion. Therefore, the combination of two materials, i.e. base and coating must be considered as an integral system to avoid hot corrosion.

Owing to the aforementioned facts, there is a significant scope in understanding the reaction kinetics and the nature of the surface scales formed during hot corrosion. The hot corrosion behavior of bare and coated alloys has not been studied extensively and is not well understood. Therefore, further studies are needed on hot corrosion behavior particularly those used for high temperature applications.

CHAPTER 2

2. LITERATURE REVIEW

The following section is a brief review of the earlier studies relevant to the present study. The literature contains a comprehensive review of the different protective coatings in molten salts. Researchers have conducted experiments to simulate real cases of hot corrosion conditions as in gas turbines, incinerators and jet engines environment to study the hot corrosion behavior.

Wu et al. [8] investigated the hot corrosion behavior of the Cr –modified aluminide coating exposed to molten salt with Ni-based superalloy DSM11 as the substrate. Hot corrosion behaviors of the DSM11 alloy, the aluminized coating and Al-Cr coating specimens were exposed to $\text{Na}_2\text{SO}_4/\text{K}_2\text{SO}_4$ (3:1) and $\text{Na}_2\text{SO}_4/\text{NaCl}$ (3:1) mixtures, at 900 °C. The exposure was done at regular intervals of 20 hours. The results showed that Cr-modified aluminide (Al-Cr) coating and aluminized coating both exhibited excellent corrosion resistance in the mixture salt of $\text{Na}_2\text{SO}_4/\text{K}_2\text{SO}_4$. Moreover, the Cr-modified aluminide coating showed good resistance in the mixture of $\text{Na}_2\text{SO}_4/\text{NaCl}$ due to the beneficial effect of Cr in the coating; while the aluminized coating was seriously damaged and lost its protective effect after corrosion.

Sidhu et al. [9] comparatively evaluated the hot corrosion behavior of the Cr_3C_2 -NiCr and Ni-20Cr coatings sprayed by HVOF on Ni-based superalloy in a molten salt environment of Na_2SO_4 -60% V_2O_5 at 900°C. The study compared coated and uncoated specimens of Superni 600. The uncoated specimen showed less resistance to hot corrosion in the molten salts due to spalling behavior of the scale. The cumulative weight gain of the uncoated specimen was more than the coated specimen. The hot corrosion resistance of the Cr_3C_2 -NiCr coating may be due to the formation of protective phases like NiO, Cr_2O_3 and NiCr_2O_4 . A rich in chromium dense oxide scale formed on the coated specimen.

In the study that investigated the behavior of the NiCrAlY coatings deposited on the Superni76 under cyclic conditions at 900 °C in $\text{Na}_2\text{SO}_4 + 60\% \text{V}_2\text{O}_5$ salt, Rana et al. [10] showed that Cr_2O_3 formed and dissolved in the corrosive salts, and spallation of

the scale was observed. There was also the formation of Al_2O_3 sublayer at the coating/scale interface which provided a corrosion resistance layer. The results further showed that during the initial cycles the salt reacted with coatings and formed a corrosive compound $\text{Ni}_3\text{V}_2\text{O}_8$ and Y reacted with vanadium to form YVO_4 . However, from cycle 100 to 200 cycles, a minimum rate of the corrosion was observed.

Lin et al. [11] conducted a study investigating high-temperature oxidation and hot corrosion behaviors of Cr_2AlC at 800-1300 °C in air. The tests were carried out in the exposure of Na_2SO_4 . The thermogravimetric-differential scanning calorimetric test revealed that oxidation began at 800 °C, which is 400 °C higher than that of other ternary transition metal aluminium carbides such as Ti_2AlC and $\text{Zr}_3\text{Al}_3\text{C}_5$. Moreover, CrAlC displayed excellent oxidation resistance, with parabolic rate constants of 1.08×10^{12} and $2.96 \times 10^9 \text{ kg}^3\text{m}^4\text{s}^{-1}$ at 800 and 1300 °C, respectively. Cr_2Al_2 exhibited good hot corrosion resistance against Na_2SO_4 salt. The basic dissolution of Cr_2O_2 lowered the basicity of the molten salt, thus stabilizing the Al_2O_3 scale.

In another study conducted by Mudgal et al. [17], Cr_3C_2 -25NiCr and Cr_3C_2 -25(NiCr)+0.4% CeO_2 coatings were deposited on nickel-based superalloy Superni 600. The study investigated the corrosion behavior of bare and coated alloys in molten salt environment (Na_2SO_4 -25%NaCl) at 900°C under cyclic conditions. Results demonstrated that bare Superni 600 corroded in the molten salt environment, with a porous scale which was accompanied by weight loss due to minor internal oxidation. Whereas the Cr_3C_2 -25NiCr and Cr_3C_2 -25(NiCr)+0.4% CeO_2 coatings developed a dense scale and an overall weight gain. Cr_2O_2 and Na_2CrO_4 were found to be the common phases in the corrosion products of bare and coated specimens.

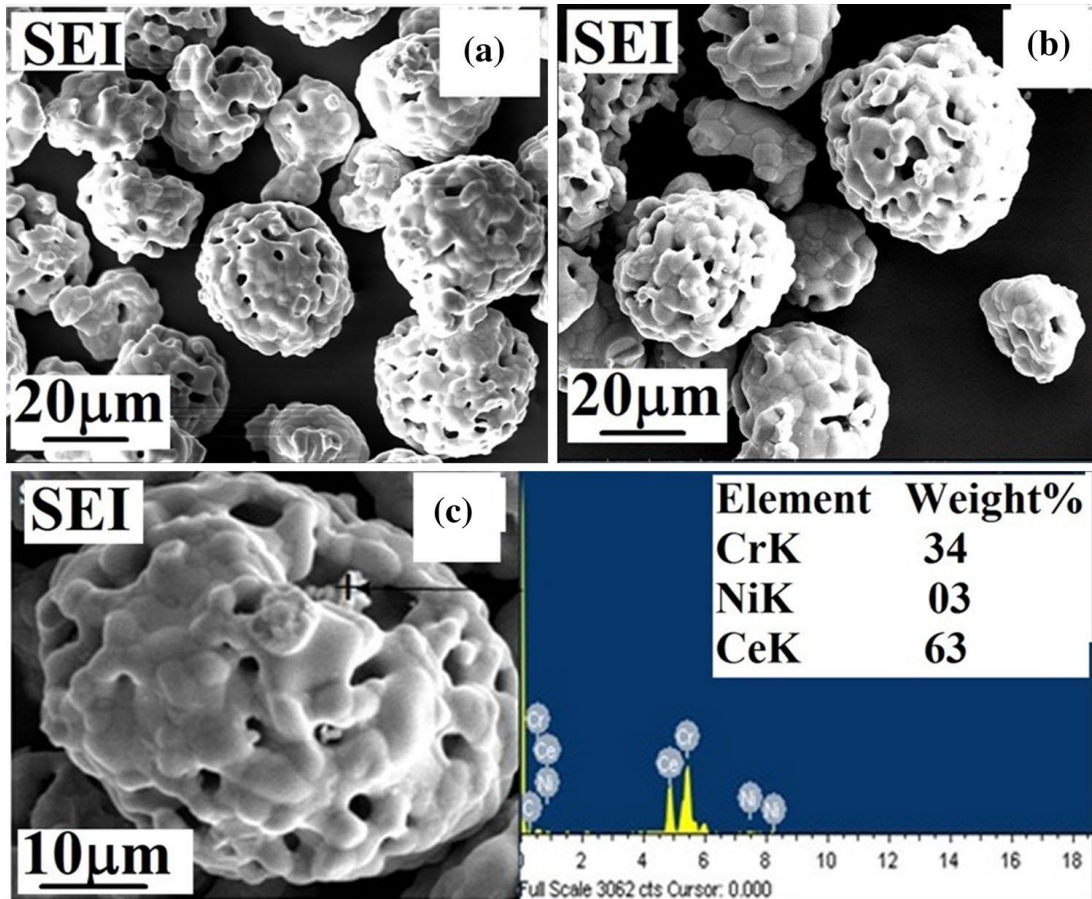


Figure 3: FESEM micrograph of coating powders (a) $\text{Cr}_3\text{C}_2\text{-25NiCr}$, (b) $\text{Cr}_3\text{C}_2\text{-25(NiCr)+0.4\%CeO}_2$, (c) $\text{Cr}_3\text{C}_2\text{-25(NiCr)+0.4\%CeO}_2$ with EDS [17]

Kamal et al. [13] deposited the coating powder $\text{NiCrAlY} + 0.4 \text{ wt.}\% \text{ CeO}_2$ on the substrates superni 75, superni 718 and superfer 800H using a detonation gun. The specimens were subject to corrosive attack in the salt mixture of $\text{Na}_2\text{SO}_4\text{-60\% V}_2\text{O}_5$ for 100 cycles under cyclic conditions. Each cycle consisted of 1 hour heating at 900°C . The results showed that there was 60 and 15% saving in overall weight gain for $\text{NiCrAlY} + 0.4 \text{ wt.}\% \text{ CeO}_2$ coated superfer 800H and superni 75 in comparison to the bare superfer 800H and superni 75. Furthermore, a dense oxide formed on the coated superalloys and hot corrosion resistance of coating could have been due to the formation of protective phases like NiO , Cr_2O_3 , Al_2O_3 , NiCr_2O_4 and NiAl_2O_4 . Formation of small amounts of oxides of iron and silicon showed diffusion from the substrate to the top surface of coating.

Mudgal et al. [14] conducted a study investigating the behavior of bare superalloys, Superni 718, Superni 600 and Superco 605, in the presence of $\text{Na}_2\text{SO}_4\text{-25\%NaCl}$.

The hot corrosion test was conducted at 900° C for 100 cycles. The Ni-based alloy 718 and alloy 600 showed a very marginal weight gain at the end of the test. However, in the case of alloy 718, NiO was seen as the major component of the scale and there is a formation of thin Cr₂O₃ layer between the scale and the substrate. This layer was capable of stopping diffusion of cation and anion species, therefore, stopping further reaction. Whereas in the case of alloy 600, the scale was thin and was mainly of Cr₂O₃, and the reacting species has penetrated through the metal layer and has reacted with the substrate. In the case of Co-based alloy, Superco 605, there was enormous weight gain accompanied with intense spalling due to the non-protective nature of the scale. The main constituents of the scale are oxides of cobalt, chromium and tungsten. The final scale consisted of only cobalt and nickel. It was concluded that Ni-based alloys are more suitable to withstand aggressive corrosive environment than Co-based alloys.

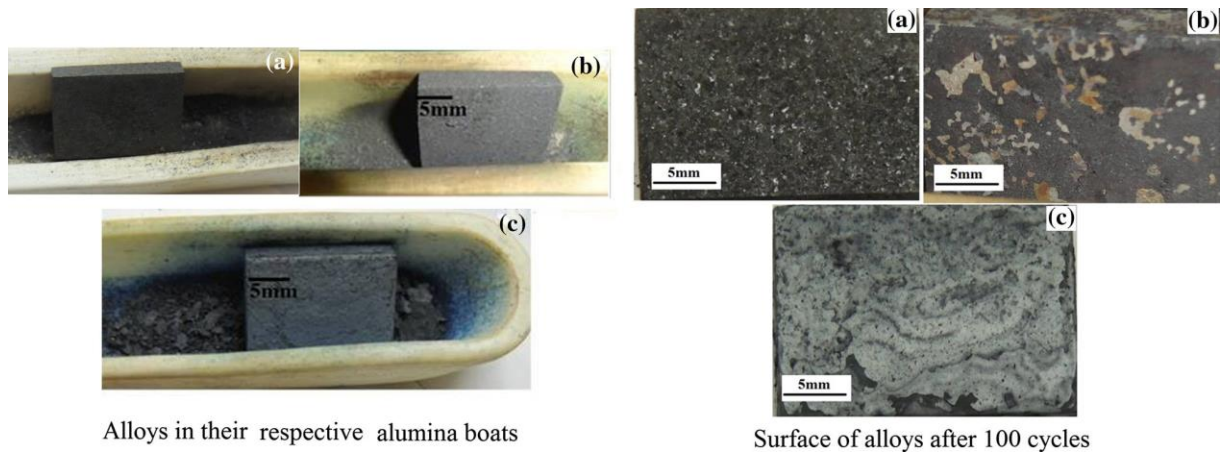


Figure 4: Macrophotos of (a) Superni 600, (b) Superni 718, and (c) Superco 605 after cyclic hot corrosion in Na₂SO₄-25%NaCl at 900° C for 100 cycles [14]

To increase the corrosion resistance of boiler components, Oksa et al. [16] applied three Ni-based coatings with high amounts of chromium were thermally sprayed on short boiler tube sections. The coatings were commercial powders, Alloy 59 (NiCr16Mo), Inconel 625 (NiCr9Mo) and NiCrAlY (NiCr10Al). The coatings were applied on a carbon steel tube (St35.8 DN 17175-79). The coatings were tested in the boiler for two years. The carbon steel tube St35.8 corroded strongly during the two year exposure in the biomass boiler. The corrosion rate was measured to be

2.3mm/year. However, the coatings had endured the boiler exposure well, the Ni-based coatings offered excellent corrosion and erosion protection to the substrate material. The extreme severe corrosion of the carbon steel was caused by chlorine induced corrosion together with the effect of potassium, copper, zinc and lead in the deposits.

To investigate hot corrosion behavior of Superfer 800H, Kamal et al. [16] exposed the superalloy substrate to two different molten salt environments $\text{Na}_2\text{SO}_4+60\%\text{V}_2\text{O}_5$ and $\text{Na}_2\text{SO}_4+5\%\text{V}_2\text{O}_5+5\%\text{NaCl}$ respectively. The test was conducted for 50 cycles at 900°C . The results showed that there was crack initiation after 10 cycles in the presence of NaCl salt. Through the cracks, molten salts attack the substrate and cause hot corrosion. The formation of protective oxide scales NiO, Cr_2O_3 and NiCr_2O_4 provided resistance to hot corrosion. During the initial cycles, the results exhibited a high nickel concentration at metal interface region and as the number of cycles increase the nickel concentration increase in scale which consists of NiO and Cr_2O_3 . Crack propagation is due to the formation of Cr_2O_3 , because the region of crack propagation showed large quantities of chromium and oxygen.

CHAPTER 3

3. METHODOLOGY

3.1. Substrate Materials

The bare alloys, boiler steel P11, P12, P22, have been procured from Kalpataru Metals & Alloys, India, in the form of rolled rectangular sheets, AISI 304SS, and substrate material of AISI 304SS. The nominal chemical composition of the materials is shown in Table 1.

Table 1: Chemical Composition of the Materials

Alloy	Chemical Composition (wt.%)											
	Fe	C	Si	Mn	S	P	Cr	Ni	Mo	Cu	Al	Ti
P11	96.60	0.13	0.71	0.50	0.013	0.023	1.30	0.09	0.47	0.13	0.023	0.007
P12	97.36	0.06	0.323	0.53	0.01	0.033	1.002	0.05	0.468	0.09	0.017	0.005
P22	94.97	0.15	0.500	0.60	0.025	0.025	2.60	-	1.13	-	-	-
304SS	66.345	0.08	1.00	2.00	0.030	0.045	20.00	10.5	-	-	-	-

3.2. Sample Preparation

- Bare alloy specimens, P11, P12 and P22, were cut into rectangular pieces of dimensions 10mm×10mm×5mm; while the coated substrate specimen was cut to the dimensions of 30mm×30mm×5mm.
- The specimens were grinded and polished using 120, 180, 240, 320 and 400 emery paper followed by alumina polishing of 0.05 μm . They were then cleaned using acetone.
- They were preheated to 300 °C for 2 hours before applying the salt solution.
- Salt solution was prepared using distilled water and 8g Na_2SO_4 + 2g NaCl + 8g K_2SO_4 + 2g KCl . A layer of salt (3-5 mg/cm^2) was applied uniformly on the preheated specimens using a camel hair brush. The specimens were dried at the temperature of 250 °C for 3 hours for good adherence of the salt on the surface.

- After drying the specimens were weighed to ensure the quantity of salt application was correct. They were kept in the boats and weight was recorded as initial measurement.

3.3. Corrosion Test

The specimens were kept in the furnace for 10 cycles under cyclic conditions. Each cycle consisted of 5 hours of heating at 900 °C followed by 20 minutes cooling at room temperature. The weights of the specimens along with the boats were recorded after each cycle; therefore spalled material fallen in the boat is included in the weight measurements. Weight change measurements are performed to know the corrosion kinetics.

3.4. Characterization Techniques

Microstructural characterization of the specimens and corrosion products was carried out by scanning electron microscope with energy-dispersive x-ray spectroscopy (SEM/EDS) in order to understand the corrosion mechanisms.

CHAPTER 4

4. RESULTS AND DISCUSSION

4.1. Results

4.1.1. Visual Observations

Surface macrographs for bare and Cr_3C_2 -NiCr coated specimens after the hot corrosion studies at 900 °C for 10 cycles in $\text{Na}_2\text{SO}_4 + \text{NaCl} + \text{K}_2\text{SO}_4 + \text{KCl}$ environment are shown in Figure 5 and Figure 6. The bare alloys showed an adherent compact corrosion scale on the surface. The oxide scale lasted up to 10 cycles, that is, no spallation was observed. The colour of the scale on the bare alloys was brownish with a mixture of grey and black phases on the surface. Cracks were also observed on the scale.

The Cr_3C_2 -NiCr coated alloy showed an intense yellow hue, particularly on the area where the salt was more concentrated. A greenish colour developed at the end of cycle 3. Mudgal et al. [18] and Rana et al. [10] reported the formation of similar oxide when Cr_3C_2 -NiCr coating is exposed to high temperatures and aggressive environment. The corrosion scale then turned greyish black with the progression of the study. Light spallation began at the end of cycle 4 (20 hours). No further spallation occurred till cycle 8, where there was great spalled material. Cracking was confined to the top edge of the specimen.

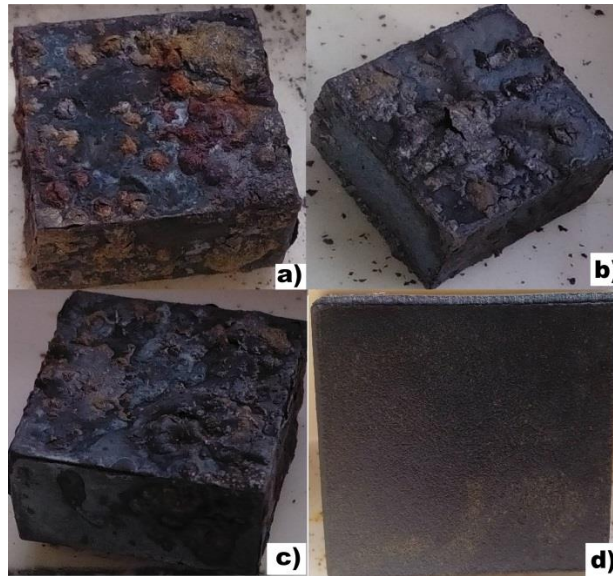


Figure 5: Macrographs of specimens after cycle 1; a) P11, b) P12, c) P22 and d) Cr₃C₂-NiCr coated specimen

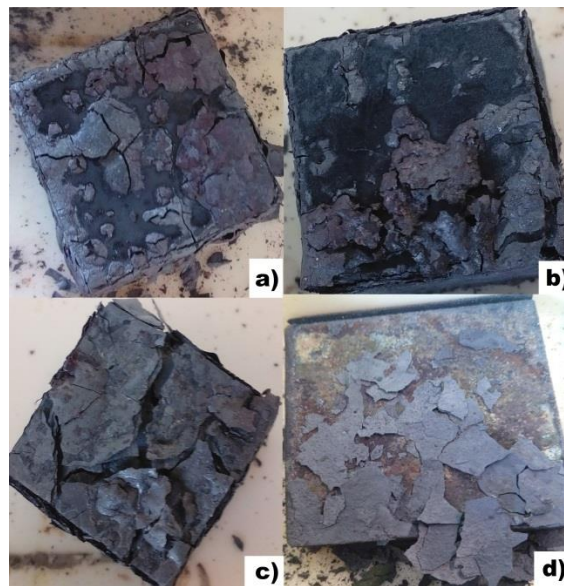


Figure 6: Macrographs of specimens at cycle 10; a) P11, b) P12, c) P22 and d) Cr₃C₂-NiCr coated specimen

4.1.2. Weight Change Measurements

Weight change (mg) vs time plot for the bare and coated specimens in Na₂SO₄ +NaCl + K₂SO₄ +KCl environment at 900 °C for 10 cycles is shown in Figure 7. Hot corroded bare specimens showed higher weight gains.

Whereas the $\text{Cr}_3\text{C}_2\text{-NiCr}$ coated specimen showed a general decline in weight measurement.

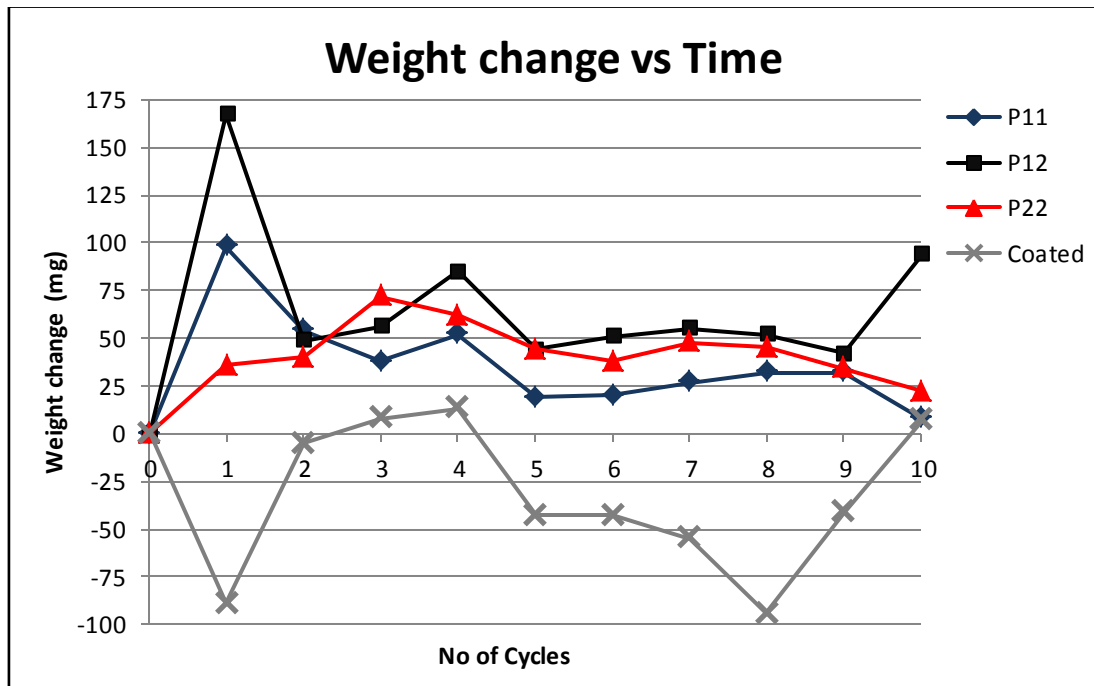


Figure 7: Weight change curves for bare and $\text{Cr}_3\text{C}_2\text{-NiCr}$ coated specimens

4.1.3. Morphology and Composition of Scales

The samples were subject to SEM-EDS analysis to characterize the surface morphology of the hot corroded specimens and the results are shown in Figure 8 to Figure 11. The microstructure of the hot corroded surface of bare P11 is shown in Figure 8. The oxide scale exhibited a dense structure with small and large globules which are irregularly distributed in the scale, with the presence of iron and oxygen as the major elements. While the microstructures of the hot corroded surfaces of bare P12 and P22, as shown in Figure 9 and Figure 10, exhibited iron and oxygen as the major elements and manganese as a minor element. The EDS analysis on the hot corroded surface scale developed on the coated specimen, as in Figure 11, indicated the presence of the elements iron, oxygen, potassium, sodium, chromium, manganese and sulfur.

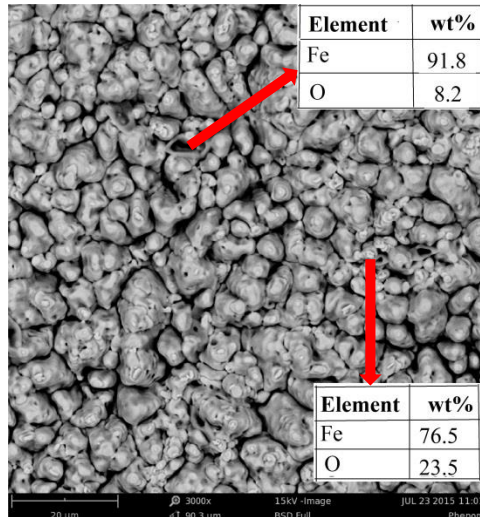


Figure 8: SEM micrograph of hot corroded bare P11 surface

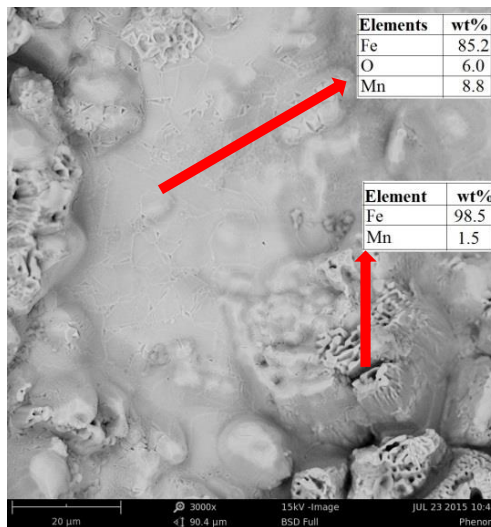


Figure 9: SEM micrograph of hot corroded bare P12 surface

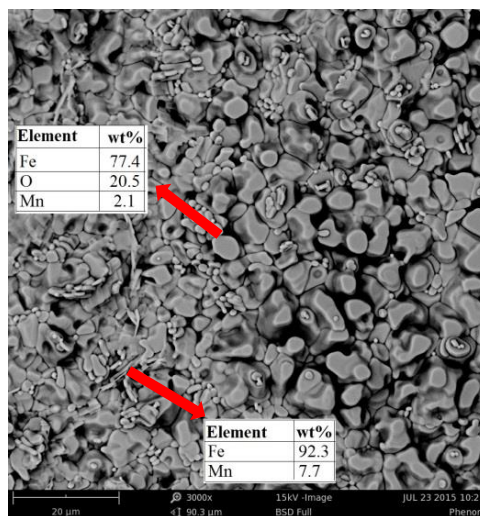


Figure 10: SEM micrograph of hot corroded bare P22 surface

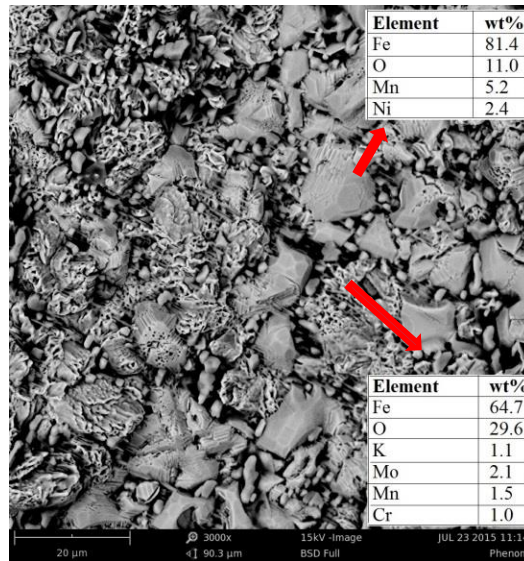


Figure 11: SEM micrograph of hot corroded $\text{Cr}_3\text{C}_2\text{-NiCr}$ coated surface

The following are the elements found on the overall hot corroded $\text{Cr}_3\text{C}_2\text{-NiCr}$ coated surface.

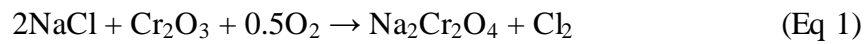
Table 2: Elements found in the hot corroded $\text{Cr}_3\text{C}_2\text{-NiCr}$ coated surface

Element Symbol	Element Name	Wt. %	Error %
Fe	Iron	65.3	0.9
O	Oxygen	20.4	1.3
K	Potassium	2.4	1.2
Cr	Chromium	2.9	1.8
Mn	Manganese	3.5	1.7
S	Sulfur	1.4	1.5
Na	Sodium	4.1	1.3

4.2. Discussion

Figure 7 shows the corrosion kinetic curves of the bare and Cr₃C₂-NiCr coated specimens. The mass change consists of a mass gain and mass loss. The mass gain is attributed to the formation of the scales, and the mass loss is caused by scale spallation and dissolution. The bare alloys demonstrated a rapid weight gain due to an accelerated formation of an oxide layer. Subsequent increase in weight was gradual as the dense oxide scale formed on the bare specimens, efficiently protecting the underlying layer from further corrosion attack. Mudgal et al. [18] reported that once the oxide formed at splat boundaries, the scale becomes dense and the diffusion of oxidizing species to the underlying sub-region gets slow which makes the weight gain and oxidation rate steady.

The Cr₃C₂-NiCr coated specimen exhibited a loss in weight during the initial cycles of the hot corrosion study. According to Mudgal et al. [17] this decrease in weight may be due to reaction between the oxide formed on the coating surface and its chlorides in the presence of oxygen as shown in Eq 1.



SEM/EDS analysis was conducted to understand the mechanism of hot corrosion on the bare and coated specimens. High amounts of Fe and O were detected on the bare hot corroded specimen surfaces which implied that Fe₂O₃ formed a solid solution. The formation of the corrosion layer is described in Eq 2. The dense solid oxide layer slowed down the hot corrosion process.



While the Cr₃C₂-NiCr coated specimen surface indicated significant amounts of Cr thus implying the formation of Cr₂O₃. The analysis also showed the amount of Na to be higher than that of Cr, which implied that at the coating surface the dissolution of Cr₂O₃ took place as seen in Eq 3 [11]; therefore causing the spallation of the top surface of the coating.



With the protective feature of the $\text{Cr}_3\text{C}_2\text{-NiCr}$ coating deteriorated during the dissolution, oxygen and sulfur could easily penetrate into the coatings and trigger the formation of internal oxides and chromium sulfides [8]. These would consequently speed up the corrosion process.

The intense spallation of the top surface of the coating may also be attributed not only to the salt attack but a combination of voids and oxygen.

CHAPTER 5

5. CONCLUSION AND RECOMMENDATION

1. Bare alloy and coated specimens were oxidized at 900 °C in the presence of $\text{Na}_2\text{SO}_4 + \text{NaCl} + \text{K}_2\text{SO}_4 + \text{KCl}$ for the exposure period of 10 cycles in order to learn the behavior of the thermal spray coating in comparison to the bare alloy.
2. The surface morphology showed the bare alloy to be prone to hot corrosion, whereas the $\text{Cr}_3\text{C}_2\text{-NiCr}$ coating morphology showed the substrate was still intact.
3. The observed corrosion resistance of the $\text{Cr}_3\text{C}_2\text{-NiCr}$ coating can be attributed to the formation of protective oxide scale Cr_2O_3 . The dissolution of the Cr_2O_3 scale by the molten salts and the presence of voids led to the intense spallation of the top surface of the coating. The top surface did not show any corrosion products, thus the coating prevented the penetration of hot corrosion to the substrate material.

Recommendation

The $\text{Cr}_3\text{C}_2\text{-NiCr}$ coating may have consisted of voids and porosity originating from the spraying process, through which the coating was mainly attacked. The porosity of the coating plays an important role as far as corrosion resistance is concerned. As a result, a denser coating would provide a better corrosion resistance, which then degrades less due to its more closely packed structure.

REFERENCES

- [1] N. Eliaz, G. Shemesh, R.M. Latanision. "Hot Corrosion in Gas Turbine Components," *Engineering Failure Analysis*, vol. 9, pp. 31-43, 2002.
- [2] *Hot Corrosion in Gas Turbines*. ASM Int. 2007.
- [3] J. Ma, S.M. Jiang, J. Gong, C. Sun. "Hot Corrosion Properties of Composite Coatings in the Presence of NaCl at 700 and 900 °C," *Corrosion Science*, vol. 70, pp. 29-39, 2013.
- [4] S.S. Chatha, H.S. Sidhu, B.S. Sidhu. "Characterization and Corrosion-Erosion Behavior of Carbide based Thermal Spray Coating," *Journal of Minerals & Materials Characterization and Engineering*, vol. 11, pp. 569-586, 2012.
- [5] I. Andijani, A.U. Malik. "Sulur and Vanadium Induced Hot Corrosion of Boiler Tubes," in *Chemistry & Industry Conference*, King Saud University, Riyadh, 2004.
- [6] H. Singh, S.S. Chatha, H.S. Sidhu, K. Sharma. "Hot Corrosion Resistance of Alloy and Composite Coatings: A Review," *International Journal of Advanced Mechatronics and Robotics*, vol. 3, pp. 85-95, 2011.
- [7] K. Yuan, R.L. Peng, X.H. Li, A. Talus, S. Johansson, Y.D. Wang. "Hot Corrosion of MCrAlY coatings in Sulphate and SO₂ Environment at 900 ° C: Is SO₂ necessarily bad?" *Surface & Coatings Technology*, vol. 261, pp. 41-53, 2015.
- [8] D. Wu, S. Jiang, Q. Fan, J. Gong, C. Sun. "Hot Corrosion Behavior of Cr-Modified Aluminide Coating on a Ni-based Superalloy," *Acta Metall. Sin. (Eng. Lett.)*, vol. 24, pp. 627-634, 2014.
- [9] T.S. Sidhu, S. Prakash, R.D. Agrawal "Hot Corrosion Studies of HVOF Sprayed Cr₃C₂-NiCr and Ni-20Cr Coatings on Nickel-based Superalloy at 900° C," *Surface & Coatings Technology*, 2006.
- [10] N. Rana, R. Jayaganthan, S. Prakash. "Stepwise Depletion of Coating Elements as a Result of that Corrosion of NiCrAlY coatings," *Journal of Materials Engineering and Performance*, vol. 23(2), pp. 643-650, 2014.

- [11] Z.J. Lin, M.S. Li, J.Y. Wang, Y.C. Zhou. "High-temperature Oxidation and Hot Corrosion of Cr₂AlC," *Acta Materialia*, vol. 55, pp. 6182-6191, 2007.
- [12] R. Kumar, V.K. Tewari, S. Prakash. "Studies on Hot Corrosion of the 2.25Cr-1Mo Boiler Tube Steel and its Weldments in the Molten Salt Na₂SO₄-60 pct V₂O₅ Environment," *Metallurgical and Materials Transaction A*, vol. 38A, pp. 54-57, 2007.
- [13] S. Kamal, R. Jayaganthan, S. Prakash. "Hot Corrosion Studies on Detonation-Gun Sprayed NiCrAlY + 0.4 wt.% CeO₂ Coated Superalloys in Molten Salt Environment," *Journal of Materials Engineering and Performance*, vol. 20 (6), pp. 1068-1077, 2011.
- [14] D. Mudgal, S. Singh, S. Prakash. "Cyclic Hot Corrosion Behavior of Superni 718, Superni 600 and Superco 605 in Sulfate and Chloride Containing Environment at 900°C," *Metallographic Microstructural Analysis*, 2014.
- [15] M. Oksa, P. Averkari, J. Salonen, T. Varis. "Nickel-based HVOF Coatings Promoting High Temperature Corrosion Resistance of Biomass-Fired Power Plant Boilers," *Fuel Processing Technology*, 125, pp. 236-245, 2014.
- [16] S. Kamal, K.V. Sharma, A.M. Abdul-Rani. "Hot Corrosion Behavior of Superalloy in Different Corrosive Environments," *Journal of Minerals and Materials Characterization and Engineering*, 3, pp. 26-36, 2015.
- [17] D. Mudgal, S. Kumar, S. Singh, S. Prakash. "Corrosion Behavior of Bare, Cr₃C₂-25%(NiCr), and Cr₃C₂-25%(NiCr)+0.4CeO₂-Coated Superni 600 Under Molten Salt at 900°C," *Journal of Materials Engineering and Performance*, vol. 23(11), pp. 3805-3818, 2014.

APPENDIX 1

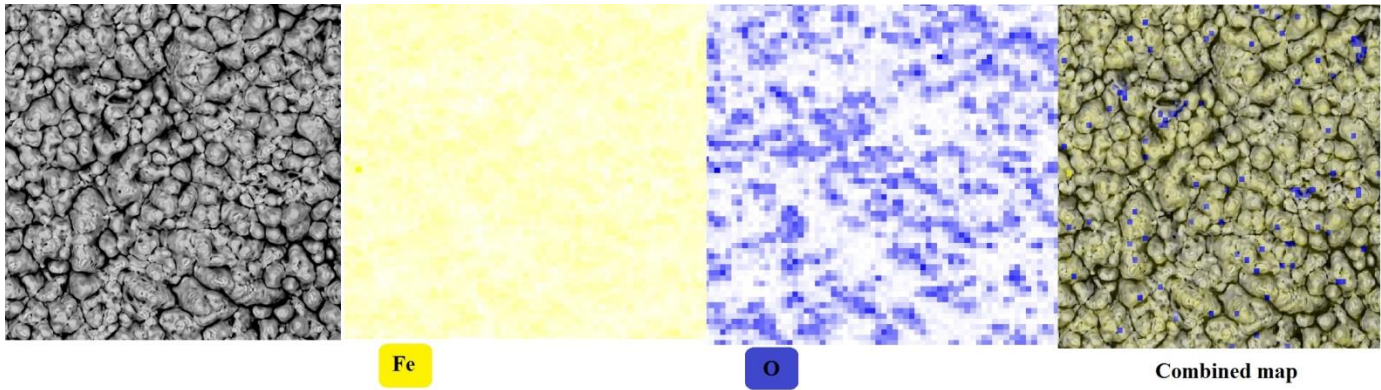


Figure 12: SEM micrographs of bare P11 hot corroded surface

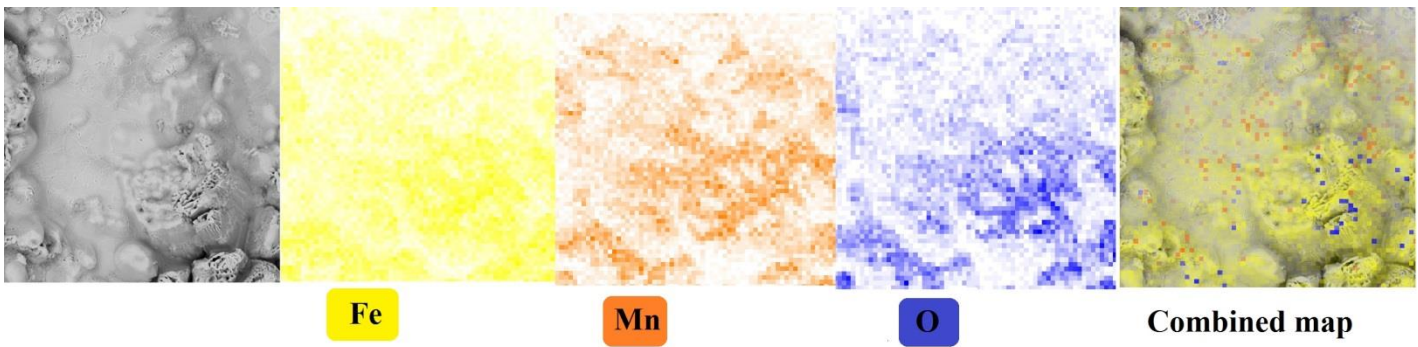


Figure 13: SEM micrographs of bare P12 hot corroded surface

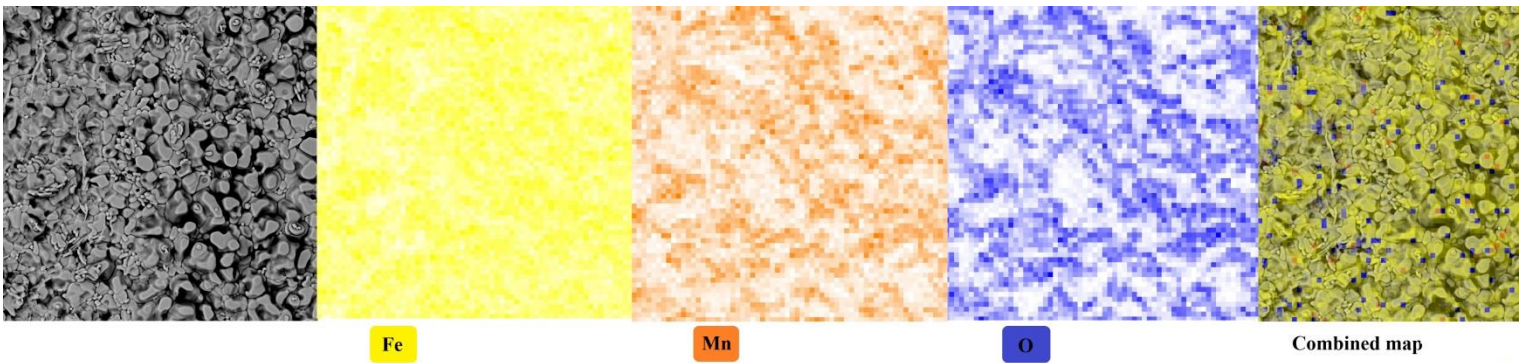


Figure 14: SEM micrographs of bare P22 hot corroded surface

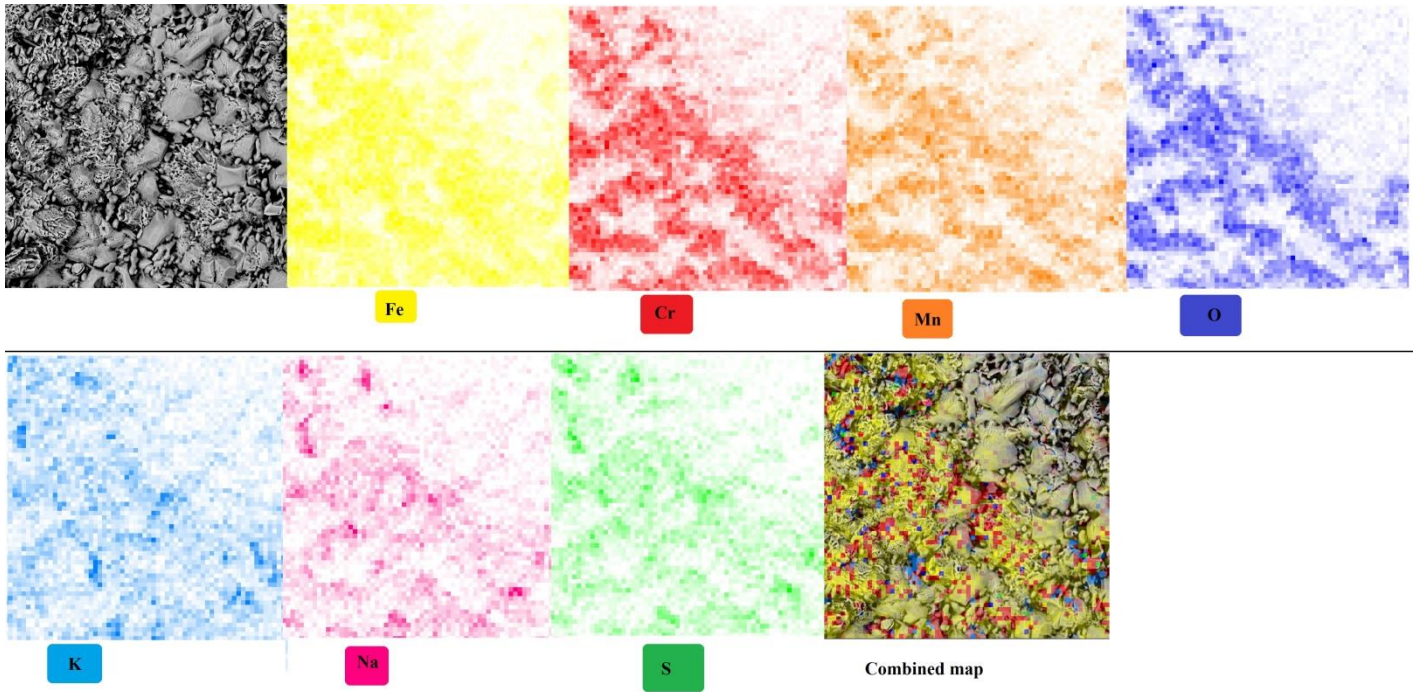


Figure 15: SEM micrographs of bare P22 hot corroded surface

APPENDIX 2

Table 3: Project Milestone for FYP I

Item/Week	1	2	3	4	5	6	7	8	9	10	11	12	13	14
Project Title Selection														
Preliminary Research and Scope Determination														
Literature Review														
Extended Proposal Submission						★								
Resource Gathering														
Proposal Defence Presentation									★					
Submission of FYP I Draft Interim Report													★	
Submission of FYP I Interim Report														★

Table 4: Project Milestone for FYP II

Item/Week	1	2	3	4	5	6	7	8	9	10	11	12	13	14
Hot corrosion test experiments														
Submission of Progress Report							★							
SEM/EDS Analysis										★				
Pre-Sedex										★				
Submission of Draft Final Report											★			
Submission of Dissertation (soft bound)												★		
Submission of Technical Paper												★		
Viva														★